Microseismic Impulses as Earthquake Precursors

G. A. Sobolev and A. A. Lyubushin

*Schmidt Institute of Physics of the Earth, Russian Academy of Sciences,
Bol'shaya Gruzinskaya ul. 10, Moscow, 123810 Russia*

Received January 30, 2006

Abstract—Records of the IRIS broadband stations in Petropavlovsk-Kamchatski, Yuzhno-Sakhalinsk, Magadan, Yakutsk, Arti, and Obninsk obtained before the Kronotskii (Kamchatka Peninsula) $M = 7.7$ earthquake of December 5, 1997, and the Neftegorsk (Sakhalin Island) $M = 7.0$ earthquake of May 27, 1995, are investigated with the use of the Spectra Analyzer interactive program, designed for the analysis of properties of scalar time series. It is found that, 5 to 10 days before the shocks, stations nearest to the sources of these earthquakes recorded pulsed vibrations a few minutes long that were separated by intervals of a few tens of minutes. The shape asymmetry of the pulses characterized by different amplitudes of positive and negative polarity phases increased toward the earthquake onset time, as did the frequency and regularity of the pulse sequence. It is assumed that the nature of this phenomenon is related to self-organization properties of the seismic process in a metastable lithosphere and to the synchronization of vibrations in the inner and outer shells of the Earth, including chaotic and quasi-periodic components.

PACS numbers: 91.30.Px

DOI: 10.1134/S1069351306090023

INTRODUCTION

The Earth is influenced by numerous oscillating fields of various origins in a wide range of periods, with some forms of energy being partially converted into others. The energy supplied to the Earth by external electromagnetic waves causes elastic vibrations due to the inverse seismoelectric effect and other types of coupling of these two forms of energy. Variations in the atmospheric pressure deform surface layers of the Earth and change the groundwater level. It has been repeatedly noted that the response of crustal rocks to external factors is time dependent. Its considerable increase is associated with nonlinear effects of the coupling of different physical fields if the geological medium is in a metastable state [Sadovsky, 1989]. The latter can be a consequence of the accumulation of tectonic stresses whose value reaches the long-term strength of rocks, which is a prerequisite of earthquakes.

The class of phenomena under discussion includes the effect of hidden periodic oscillations arising before a strong earthquake in the flux of weak seismic signals [Sobolev, 2003, 2004]. It is assumed that the source region in a metastable state is more sensitive to external factors within a specific range of periods (for example, within the range of resonance maximums of elastic vibrations of blocks or layers of the lithosphere). Sobolev et al. [2005] showed that a periodicity in the flux of microseisms is related to vibrational pulses a few minutes in length following each other with an interval of a few tens of minutes. The present paper is devoted to a detailed study of the properties of such variations.

METHODOLOGY

We studied Z-component records of IRIS seismic stations of the same type in Petropavlovsk-Kamchatskii (Pet), Yuzhno-Sakhalinsk (Yss), Magadan (Mag), Yakutsk (Yak), Arti (Aru), and Obninsk (Obn), whose location is shown in Fig. 1. The initial data, kindly provided by the Geophysical Service of the Russian Academy of Sciences, consisted of series of discrete values of the vibration velocity of pedestals (nm/s) with a downsampling rate of 0.05 s. A typical spectrum of the recorded vibrations was shown in [Sobolev et al., 2005]. Vibrations recorded in the short-period (seconds) range of the spectrum were mainly produced by earthquakes and microseisms of the oceanic origin. In this range, the power of spectral oscillations decreased toward longer periods. The long-period range (hours) included vibrations caused by the earth tides and their overtones; here, with increasing periods, the spectral power increased up to peaks at periods of 12 and 24 h. The intermediate range of periods from 6 to 60 min, located in the region of the spectral power minimum, is the main object of study in the present work. This range, including the natural vibrations of various layers of the Earth [Zharkov and Trubitsyn, 1980], was commonly studied only within short time intervals after strong earthquakes. We had the opportunity to examine the properties of vibrations in this range recorded at the aforementioned stations during a month before two strong earthquakes: the Kronotskii (Kamchatka Peninsula) December 5, 1997, $M = 7.7$ and the Neftegorsk (Sakhalin Island) May 27, 1995, $M = 7.0$ earthquakes. The location of their epicenters is shown in Fig. 1. In
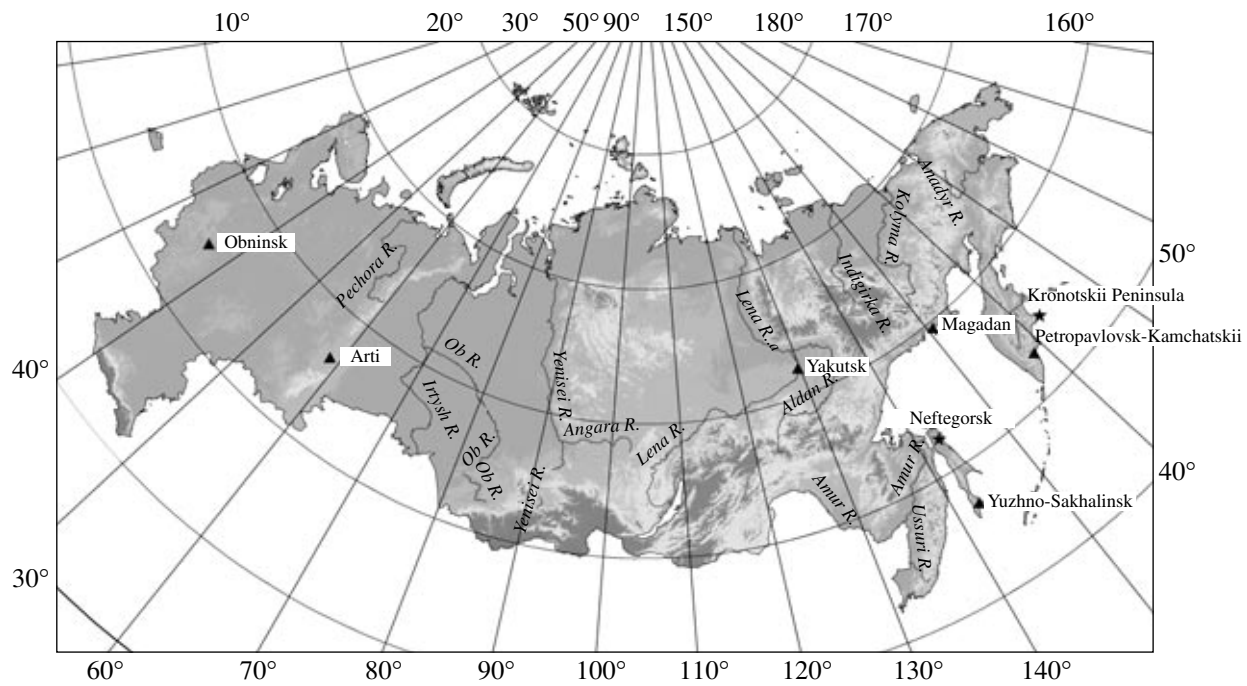
Fig. 1. Position of the IRIS stations whose records were analyzed before the Kronotskii (Kamchatka Peninsula) and Neftegorsk (Sakhalin Island) earthquakes. The epicenters of the earthquakes are shown by stars.

the previous paper [Sobolev et al., 2005], primary attention was given to the search for hidden periodic variations in the flux of microseisms and the analysis of records of the Pet station, which was the nearest to the epicenter of the Kronotskii earthquake, revealed that vibrations with a period of 37 min absent in records of farther stations arose three hours before the earthquake. It was also demonstrated that, a few days before the earthquake, this station recorded vibrations in the form of asymmetric pulses of unknown origin. The authors assumed that the sequence of these pulses was responsible for the periodic component. In the present work, we tried to examine this phenomenon in more detail, and this required additional software tools. A.A. Lyubushin has developed the Spectra Analyzer interactive program for the data mining of properties of scalar time series; a brief description of his program is given below.

The program, written in Visual Basic, realizes the user interface with a graphic display of all intermediate results, enabling interactive data analysis without leaving the interface. All computations are carried out by a dynamic link library written in Compaq Visual Fortran and including numerical procedures of spectral analysis, wavelet packet expansions, extraction and elimination of a trend, and so on. The computer program performs the following operations for scalar time series:

estimation of the power spectrum by the Burg maximum entropy method and averaging of periodograms;

estimation of the trend and its elimination with the help of smoothing by Gaussian kernels with a given scale of averaging or by local polynomials of a given order (from 0 to 10) in moving windows of a given radius;

bandpass filtering of a time series, extracting the harmonics with frequencies in a chosen band;

estimation of the evolution of the logarithmic power spectrum in the moving time windows of a given width (Burg's evaluation in each window);
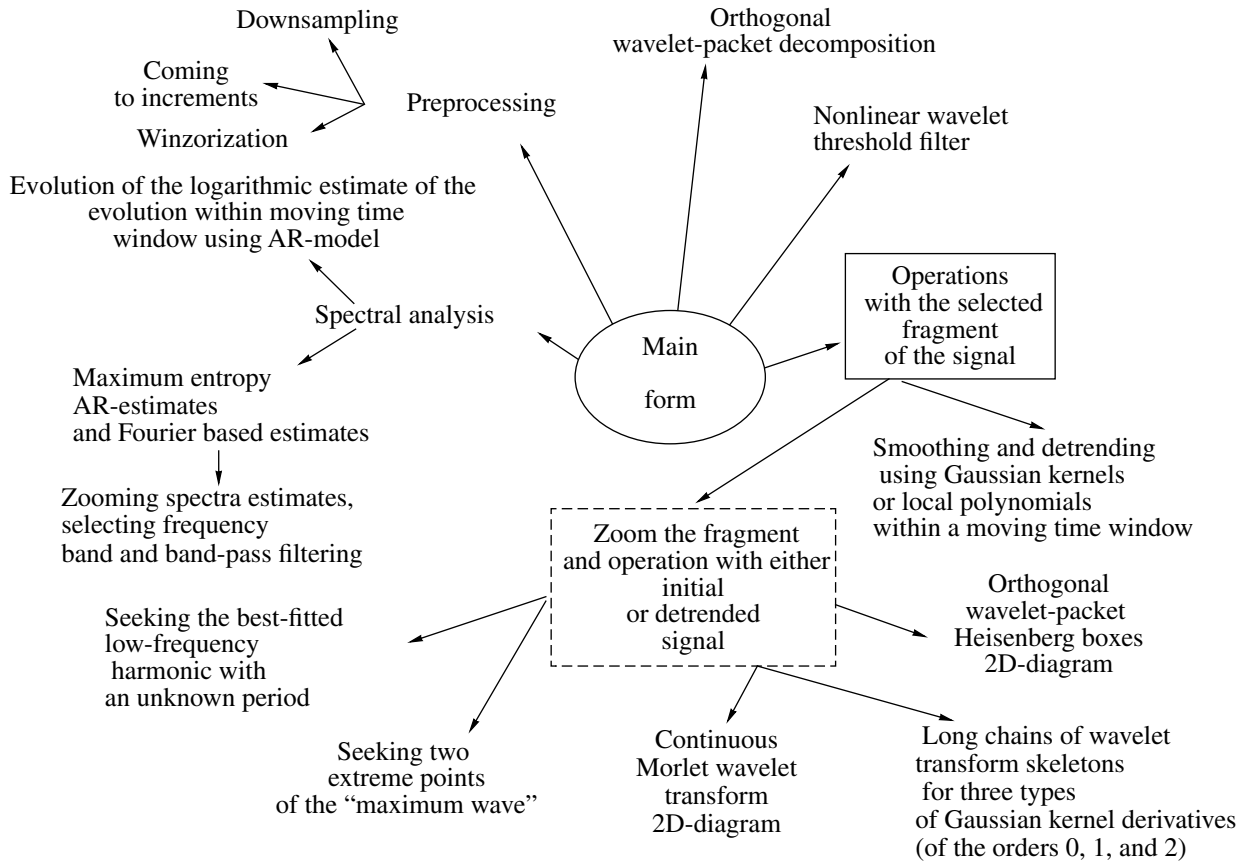
orthogonal wavelet packet decomposition of a signal with the splitting of each detail level by 1 (the ordinary orthogonal decomposition), 2, 4, or 8 times;

nonlinear threshold wavelet filtering with an optimum wavelet and the Donoho–Johnston threshold or with another wavelet and a signal compression ratio chosen by the user;

identification of long chains of the skeleton of maximum moduli of continuous wavelet transforms using the first and second derivatives of the Gaussian kernel;

calculation of the frequency–time diagram of the logarithmic squared modulus of a continuous wavelet transform with the complex-valued Morlet wavelet;

calculation of the frequency–time diagram of the logarithmic squared moduli of orthogonal wavelet transform coefficients with the splitting of each detail level by 1 (the ordinary orthogonal expansion), 2, 4, or 8 times (the Heisenberg boxes);

Downsampling

Coming
to increments

Winzorization

Preprocessing

Orthogonal
wavelet-packet decomposition

Nonlinear wavelet
threshold filter

Evolution of the logarithmic estimate of the
evolution within moving time
window using AR-model

Spectral analysis

Main
form

Operations
with the selected
fragment
of the signal

Maximum entropy
AR-estimates
and Fourier based estimates

Zooming spectra estimates,
selecting frequency
band and band-pass filtering

Smoothing and detrending
using Gaussian kernels
or local polynomials
within a moving time window

Zoom the fragment
and operation with either
initial
or detrended
signal

Orthogonal
wavelet-packet
Heisenberg boxes
2D-diagram

Seeking the best-fitted
low-frequency
harmonic with
an unknown period

Seeking two
extreme points
of the "maximum wave"

Continuous
Morlet wavelet
transform
2D-diagram

Long chains of wavelet
transform skeletons
for three types
of Gaussian kernel derivatives
(of the orders 0, 1, and 2)

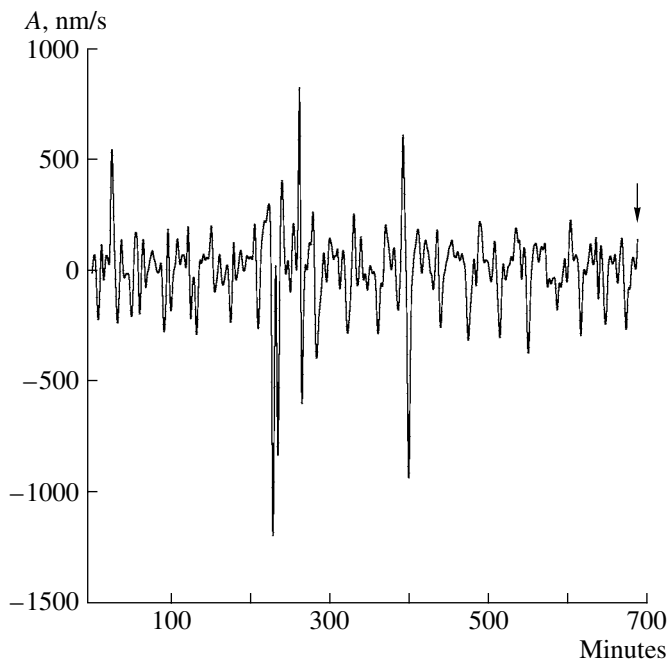**Fig. 2.** Block diagram of the user interface of the Spectra Analyzer computer program.
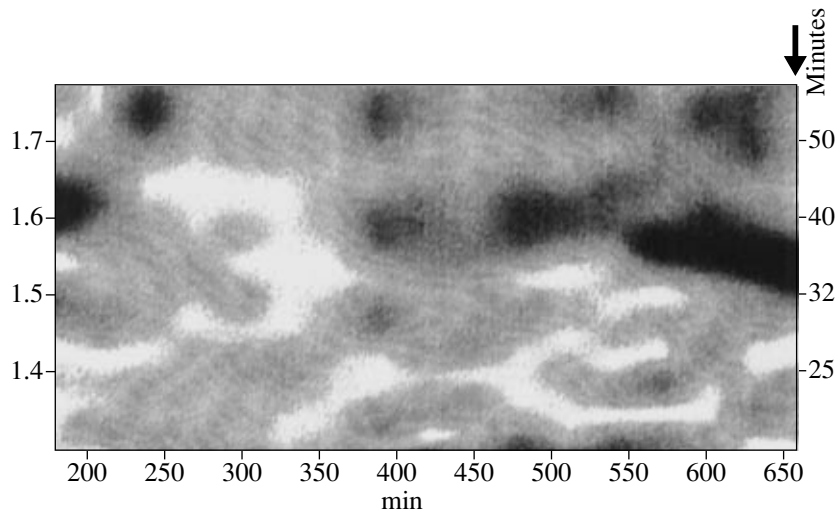
Fig. 3. Spectral time diagram of the increment of the logarithmic likelihood function $\Delta \ln L$ obtained from the analysis of the December 5, 1997, Pet record. The period (in minutes) of the spectrum and the logarithm of this period are laid off on the right and left ordinate axes, respectively. The occurrence time of the Kronotskii ($M = 7.7$) earthquake is shown by the arrow.

fitting of a time series of a low frequency harmonic with an unknown period found by the minimization of the residual variance;

a search for the extreme points, period, and amplitude of a maximum pulsation in the chosen fragments.

In addition, the program can perform the following preprocessing operations:

transition to a larger interval of sampling whose length is increased by either a whole or a fractional (greater than unity) number of times. In the case of an

A, nm/s

increase by a whole number of times, the successive averages of a given time series are calculated using time windows of widths of 2, 3, 4, etc., samples, and the variance (the unbiased sample estimate) of the deviations of the initial series from these successive averages is simultaneously calculated and written in a special file; in the case of an increase by a fractional number of times (greater than unity), the transition is accomplished with the help of the Fourier transformation, suppression of harmonics with periods higher than the new Nyquist frequency, inverse Fourier transformation, and linear interpolation within the initial sampling time step;

transition to the time series of increments;

iterative clipping of large outliers by the so-called winzorization technique: the calculation of the mean $\bar{x}$ and the standard deviation σ and the truncation of time series values lying beyond the levels $\bar{x} \pm 4\sigma$; this succession of three operations is repeated until the values $\bar{x}$ and σ stop varying;

calculation of the variance of the initial or transformed series.

A block diagram of the user interface of the program is presented in Fig. 2.

Since the operations of trend estimation and elimination are vital to the description of the method used for obtaining the main result in our paper, we give their brief description. Let $X(t)$ be an arbitrary bounded integrable signal continuous in time. We define the kernel

averaging with the scale parameter $H > 0$ as the mean $\bar{X}(t|H)$ at the time t calculated by the formula

$$\bar{X}(t|H) = \int_{-\infty}^{+\infty} X(t + H\xi)\psi(\xi)d\xi / \int_{-\infty}^{+\infty} \psi(\xi)d\xi, \quad (1)$$

where $\psi(\xi)$ is an arbitrary nonnegative bounded symmetrical integrable function called the averaging kernel [Hardle, 1989]. If $\psi(\xi) = \exp(-\xi^2)$, the value $\bar{X}(t|H)$ is called here the Gaussian trend with the averaging parameter (radius) H. For signals with a discrete time, the kernel trends can be effectively calculated with the help of the fast Fourier transformation.

RESULTS

The great length of the initial data series required a modernization of the method that we previously applied to the analysis of hidden periodicities in a sequence of pulses (on the basis of the identification of maximums of the logarithmic likelihood function increment $\Delta \ln L$) [Lyubushin et al., 1998; Sobolev, 2004; Sobolev et al., 2005]). The new software allows the initial series to be analyzed without the preprocessing of the series or after its aggregation to a sampling level of 1 s. This considerably accelerated the analysis procedure. Figure 3 presents the spectral time diagram $\Delta \ln L$ obtained by the processing of the Pet record of December 5, 1997 (the 339th day of the year) after a decrease of the sampling interval to 1 s, winzorization of the initial series, suppression of the high frequency component within the range of periods of a few seconds, and elimination of the low frequency trend with the help of the Spectra Analyzer program described above. The arrow indicates the time moment of the Kronotskii earthquake. During the last 120 min before this earthquake, periodic variations within a range of 40 to 33 min are observed. The diagram was calculated with a moving window 180 min wide at a step of 30 min, so that the beginning of the diagram (180 min) coincides with 03:00 GMT on December 5. The record used for calculating this is shown in Fig. 4 and naturally begins at 00:00 GMT on December 5.

Two features that become clearly recognizable with approaching the time moment of the earthquake are observed in Fig. 4: (1) pulses of negative polarity relative to the zero line become higher in amplitude than pulses of positive polarity and (2) successive pulses arise regularly (every ~30–40 min), with the time between them somewhat shortening during the last 100 min. The comparison of Figs. 3 and 4 suggests that the periodicity of variations in the diagram in Fig. 3 is caused by the regular occurrence of the pulses observed in the time series in Fig. 4.

Inspection of records within the interval from November 4 to December 5, 1997, showed that the number of pulses per unit time of the type observed in Fig. 4
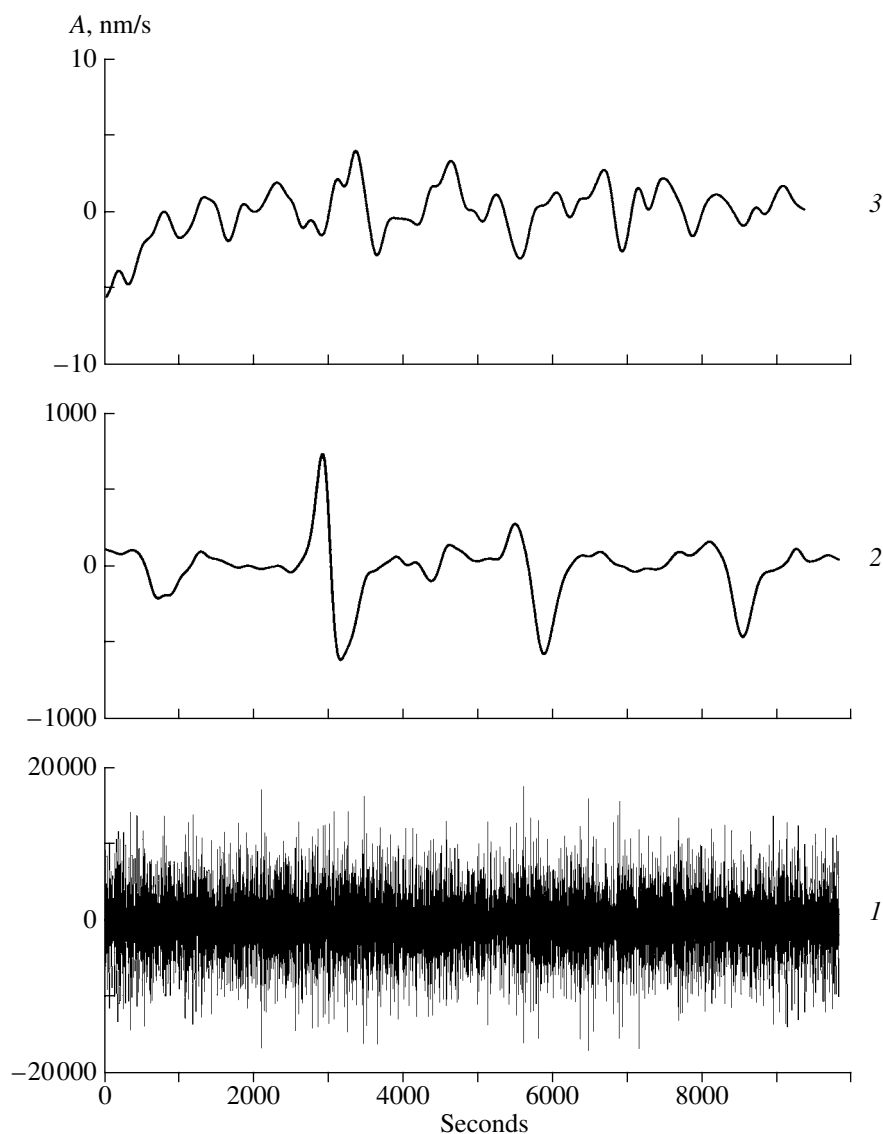
Fig. 5. Fragments of Pet (*1, 2*) and Obn (*3*) records before the Kronotskii earthquake: (*1*) initial record; (*2, 3*) variations within the range of periods of the order of minutes.

increased about 5 days before the Kronotskii earthquake. A series of short intervals of the record was analyzed in detail for comprehensive study of its structure. Plots *1* and *2* in Fig. 5 represent the same interval about 3 h long of the Pet record of December 3. Plot *1* is the record discretized at a rate of 1 s, and it is filled with microseismic variations of a 1-s range of periods. Plot *2* is the low frequency component extracted after the suppression of high frequencies by means of smoothing by Gaussian kernels with an averaging radius of 100 s. The pulses observed in this plot exhibit the following features: (1) each of the pulses is ~10–15 min long, and they are separated by intervals of ~40 min; and (2) the pulse shape varies from nearly symmetrical to unipolar, with the positive phase being gradually suppressed. Note that the pulse amplitude in plot *2* is an order of magnitude lower than the level of microseisms in plot *1*

and this is why they are unrecognizable in plot *1*. For comparison, Fig. 5 presents a fragment of an Obn record similarly processed in the same time interval (plot *3*); the Obn station is located on the Eastern European platform at a distance of 6500 km from Pet (see Fig. 1). Pulses of the type of plot *2* are not observed, but the amplitude of the variations is two orders of magnitude lower.

The next step was the processing of the sequence of pulses in the interval 1 month long immediately preceding the Kronotskii earthquake. For this purpose, a computer program was designed for their automatic extraction. Since the pulses of interest belong to the intermediate range of periods, we had to increase the length of the sampling interval from the initial value of 0.05 s to 1 s and then eliminate the low frequency influence (includ-
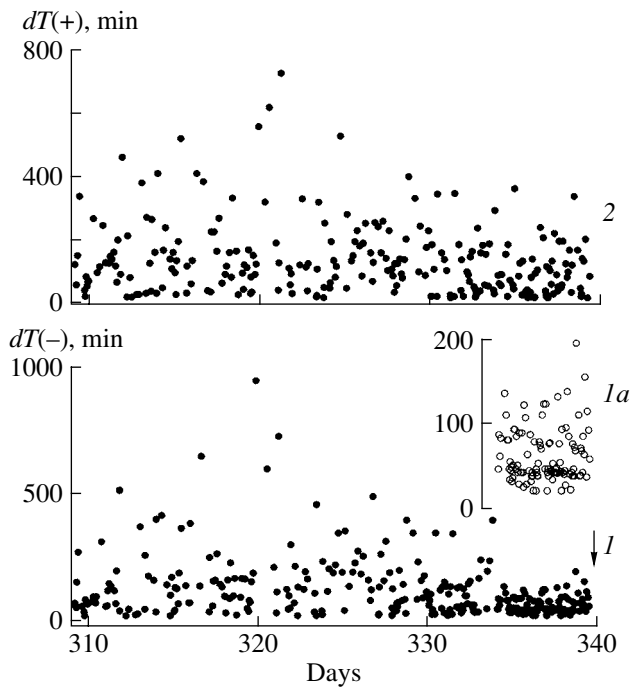
Fig. 6. Sequence of the time intervals *dT* between successive pulses before the Kronotskii earthquake: (*1*) negative polarity; (*2*) positive polarity; (*1a*) scanning with a higher resolution in amplitude. Day numbers of the year 1997 are laid off on the abscissa axis; the arrow shows the occurrence time of the Kronotskii earthquake.

ing the tidal effect) on the record and, after the transition to the 1-s sampling, the higher frequency noise as well. These preliminary operations were accomplished by the averaging and downsampling of the record by 20 times, removal of the low frequency Gaussian trend with the scale parameter $H = 1000$ samples (seconds), and subsequent calculation of the Gaussian trend with the parameter $H = 100$ s. We emphasize that the trend is first removed with $H = 1000$ s and deviations from the trend are then removed with $H = 100$ s.

A 1-s sampled signal resulting from these preliminary operations has a power spectrum lying in the range of periods of about 200 to 2000 s. Note that we could obtain the same result by the ordinary bandpass Fourier filtering, but the Gaussian trends are preferable: with their application, the side effects due to the steepness of the frequency filter do not arise and, moreover, it is easier to eliminate the edge effects caused by the finiteness of the sample filtered. High amplitude pulses should be identified automatically in the resulting signal. An expansion in the Haar wavelets [Mallat, 1998] is most suitable for this purpose. Namely, after the direct Haar wavelet transformation, only a small preset portion $(1 - \alpha)$ of wavelet coefficients maximal in modulus was left, while all the other coefficients were set to zero (the positive parameter $\alpha < 1$ can be called the compression level). The inverse wavelet transformation was further applied, providing a sequence of pulses of a fairly high

amplitude that are usually separated from each other by intervals of constant values previously filled with noise. In the wavelet analysis, this operation is known as denoising. The choice of the Haar wavelet for this operation was dictated by the simplicity of the subsequent automatic extraction of rectangular pulses. The choice of the compression level α controls the number of pulses extracted and the degree of noise suppression. We should note that a signal processed in this way already contains a rather large number of wavelet coefficients that are close or even equal to zero simply because this signal was obtained by the preliminary operations of elimination and extraction of trends. Moreover, it is obvious that the compression level also depends on the sample length because a greater sample yields a greater number of coefficients. We processed series by portions in intervals 1 day (86 400 1-s samples) long. The compression level was set equal to 0.9995, which yielded about 43 pulses per day; additional selection criteria were then applied to these pulses (see below).

Figure 6 plots the time (*dT*) between successive pulses of negative (–) and positive (+) polarity in the interval from November 4 (the 309th day of the year) to December 5 (the 339th day of the year). The calculations included pulses whose amplitude was larger than $1m$, where m is the median of their distribution, and with $dT > 20$ min. The latter condition was due to the need to exclude from the analysis quasi-periodic low frequency variations, arising in records after strong far earthquakes.

Plot *1* demonstrates that, five days before the Kronotskii earthquake, a considerable (hundreds of minutes) scatter in the times reduces to tens of minutes. A more detailed scanning of the amplitude of *dT* (inset *1a*) reveals a chain in the interval ~50–30 min, indicating not only a shortening of the intervals between successive pulses but also a regular pattern of their occurrence. Thus, the analogy with the features observable in Figs. 3 and 4 is evident. This phenomenon is not so well expressed in the structure of pulses of positive polarity (plot *2* in Fig. 6).

A decrease in length of intervals between successive pulses should correspond to an increase in their number per unit time. The question arises whether this could be due to the increase of the level of "ordinary" microseisms of a 1-s range of periods caused by sea waves or the wind. Plot *1* in Fig. 7 shows the level of microseisms in terms of the variance of the initial record D (see plot *1* in Fig. 5) calculated in successive windows 4 s wide (80 initial samples with a sampling frequency of 20 Hz).

Plots *2* and *3* in Fig. 7 demonstrate the variations in the number of pulses of positive and negative polarity during 1 day with a step of 0.1 day. A gradual increase in the number of pulses of negative polarity $N(-)$ before the earthquake noncorrelating with the amplitude of microseisms is evident. However, the local maximums
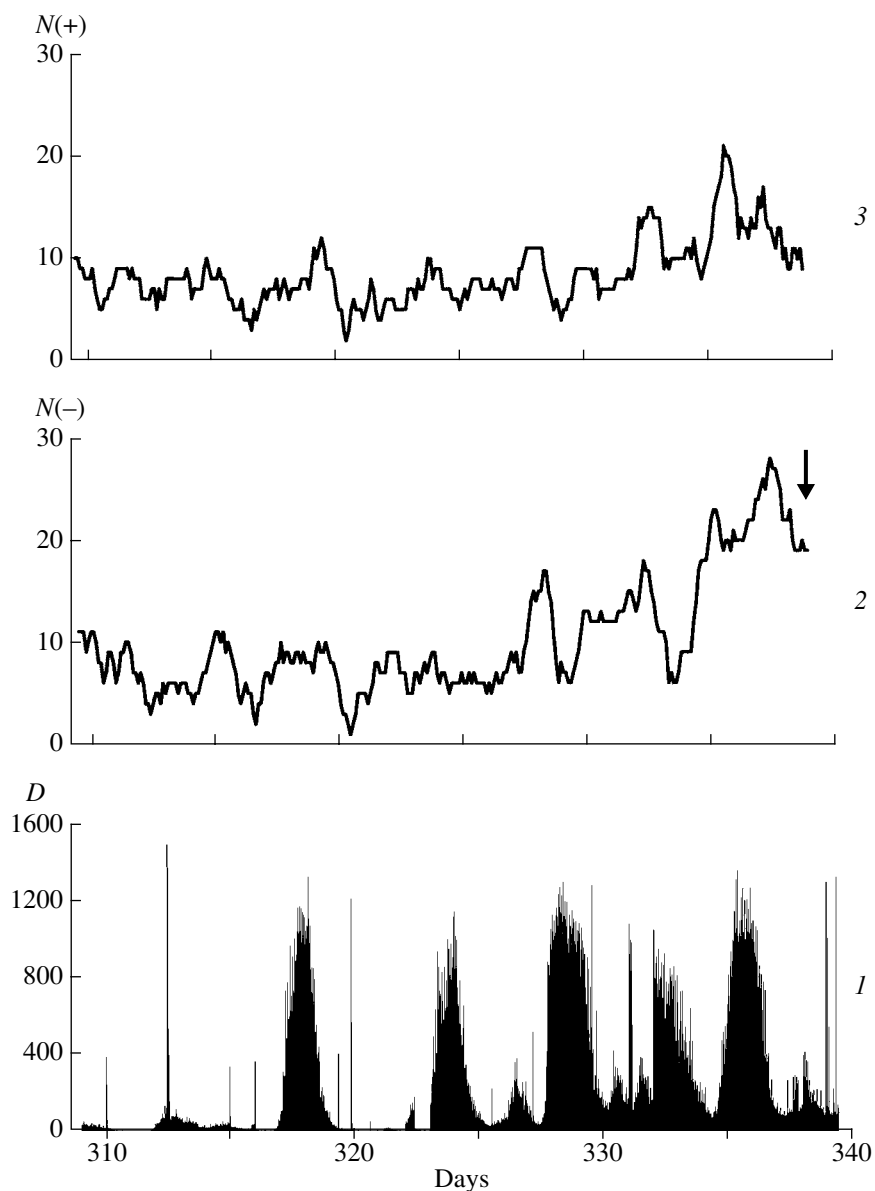
Fig. 7. Comparison of the microseismic level in the range of periods of the order of seconds (*1*) with the daily number of pulses of negative (*2*) and positive (*3*) polarities. The day numbers of the year 1997 are laid off on the abscissa axis; the arrow shows the occurrence time of the Kronotskii earthquake.

$N(+)$ on the 333rd and 336th days coincide with the rise in the microseismic level, leaving open the question about their cause–effect relation. Curves *2* and *3* are artificially shifted to the left by 0.5 day for the convenience of their comparison with the microseismic level because, with a summation window of 1 day, their initial points relate to the end of the 309th day. Note also that, during the 2 days before the earthquake, the numbers of pulses $N(-)$ and $N(+)$ and the microseismic level did not rise.

Now, we consider the situation before the Neftegorsk earthquake on May 27, 1995. The whole procedure of record processing was similar. Figure 8 presents a record fragment of microseisms observed at the Yss station (plot *1*) and the low frequency components of the Yss (plot *2*) and (for comparison) Obn (plot *3*) records. Both asymmetric and symmetric pulses ~10–15 min long are observed in plot *2*. The comparison of Fig. 8 (the Neftegorsk earthquake) and Fig. 5 (the Kronotskii earthquake) leads to the following conclusions: the pulse lengths in both cases coincide (plot *2*); unlike the Kronotskii earthquake, the intervals between successive pulses before the Neftegorsk earthquake are irregular; the pulse amplitude in Fig. 8 is about 20 times lower as compared with Fig. 5; the amplitude of microseisms (plot *1* in Fig. 8) is about 25 times lower than in Fig. 5; and the oscillations recorded at the Obn station (plots *3*) in both cases are comparable in ampli-
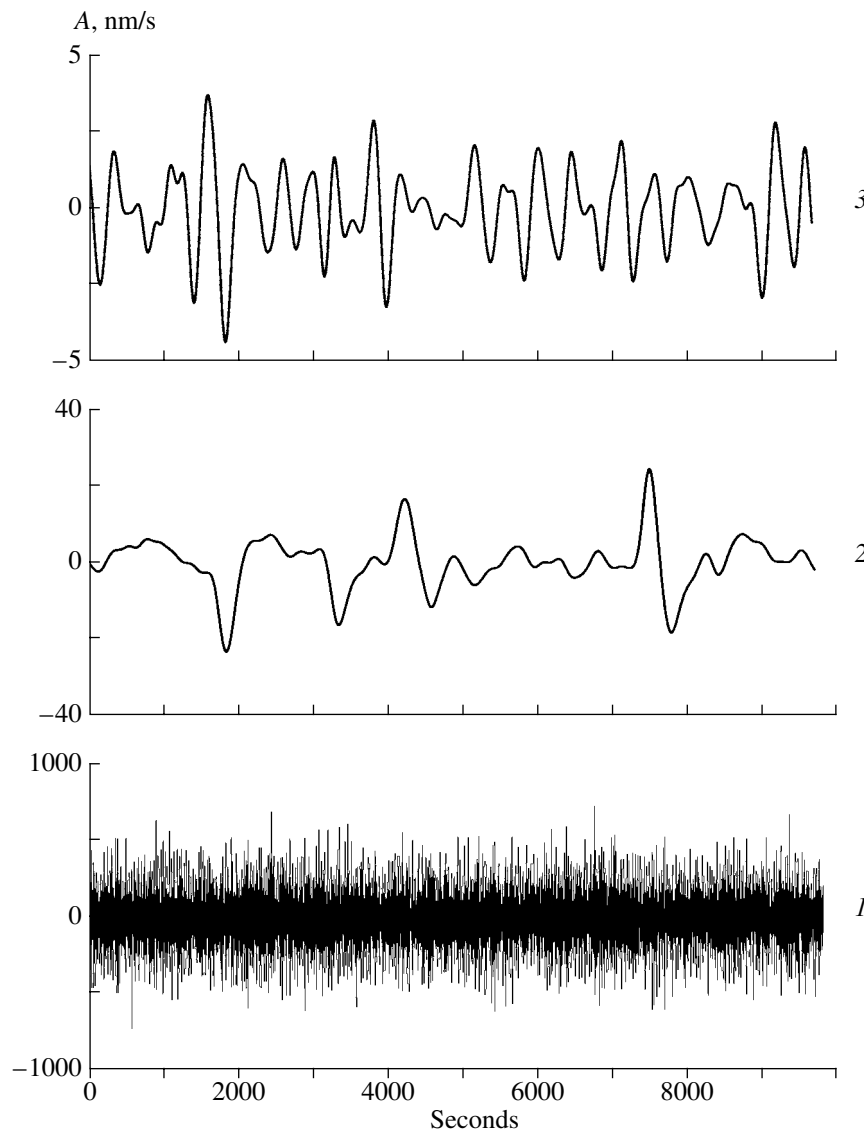
Fig. 8. Fragments of Yss (*1, 2*) and Obn (*3*) records before the Neftegorsk earthquake: (*1*) initial record; (*2, 3*) variations within the range of periods of the order of minutes.

tude (~5–7 nm/s), but they differ in structure from the oscillations recorded at the Yss and Pet stations.

Figure 9 presents the plots of the times (*dT*) between successive pulses of negative (–) and positive (+) polarities in the interval from May 1 to May 27, 1997 (the 121st–127th days of the year). Plots *1* and *2* demonstrate that, 10 days before the Neftegorsk earthquake, a considerable (hundreds of minutes) scatter in the times reduces to tens of minutes. The following distinctions from the Kronotskii earthquake (Fig. 6) are noticeable: the *dT* interval started to decrease 10, rather than 5, days before the earthquake, and this decrease was characteristic of pulses of both negative and positive polarities; the 10-day interval of a shorter interpulse time consists of two subintervals separated by a period of a larger scatter in *dT* values; and regularly recurring

pulses that could cause maximums in the spectrum of vibrations are not observed (inset *1a*).

Figure 10 compares the level of microseisms (plot *1*) with the number of low frequency pulses (*2* and *3*) for the Yss station. The increase in the number of pulses of negative polarity $N(-)$ in the last five days before the Neftegorsk earthquake does not correlate with the amplitude of microseisms. The maximums of $N(-)$ and $N(+)$ within the interval 137–142 days coincide in time with a rise in the microseismic level. The comparison of the data from the Neftegorsk (Fig. 9) and Kronotskii (Fig. 6) earthquakes suggests that only the pulses of negative polarity $N(-)$ demonstrate a distinct increase in their number per unit time in the latter five days before each of the events and the number of pulses of

both positive and negative polarity in both cases does not exceed a few tens per day.

DISCUSSION

Based on the data of the present study and taking into account results obtained in [Sobolev, 2004; Sobolev et al., 2005], the following three main results are noteworthy. (1) A few days before the Kronotskii and Neftegorsk earthquakes, pulses of seismic vibrations arose within a range of periods of the order of minutes and had amplitudes an order of magnitude lower than the microseisms within a range of periods of the order of seconds. (2) The time intervals between successive pulses shortened with approaching the earthquake and, in the case of the Kronotskii earthquake, they are observed to occur regularly with a period of the order of 30–40 min. (3) With the approach of the earthquake occurrence time, the number of asymmetric pulses increased. Below, we discuss the possible origins of these three phenomena.

Regular occurrence of pulses in the range of periods of the order of several minutes. After the global system of broadband seismic stations had been created at the end of the 1990s, a number of publications were devoted to seismic noises within a range of 10^{-2}–10^{-3} s. Thus, Tanimoto et al. [1998] attributed the occurrence of the vibrations in the solid Earth to the effect of variations in the atmospheric pressure. Kobayashi and Nishida [1998] proposed an alternative hypothesis according to which the vibrations are excited by multiple weak earthquakes whose energy lies below the sensitivity threshold of seismic stations. It was shown in these and other studies that vibrations of the range of periods of several minutes exist virtually constantly, including time intervals free from strong earthquakes. However, sequences of separate pulses similar to those observed in our case, apparently, have not been revealed. Possibly, this is due to the fact that the majority of researchers applied the technique of the Fourier spectral analysis, which is not adapted to the study of a transient process consisting of pulsations of various amplitudes and lengths. The application of the versatile software package (including the wavelet analysis) described above has proven highly effective.

The factors responsible for the occurrence of pulses can lie either outside or inside the solid Earth. The processes in the outer shells of the Earth (the atmosphere and ionosphere) include both chaotic and quasi-periodic components. We will proceed from the assumption that the dissipative system of the lithosphere is in a metastable state (particularly, before an imminent strong earthquake) and its inner processes possess the properties of deterministic chaos [Nikolis and Prigogine, 1977]. Let the time (t) variations in dynamic cha-
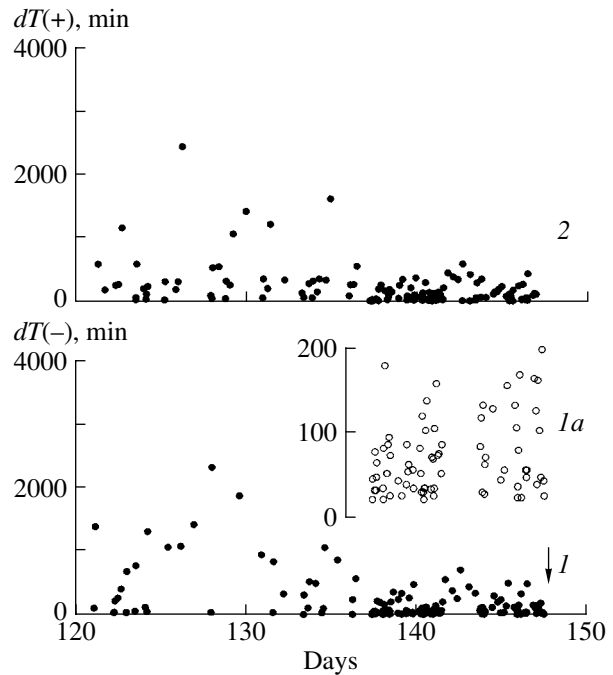
Fig. 9. Sequence of the time intervals dT between successive pulses before the Neftegorsk earthquake: (*1*) negative polarity; (*2*) positive polarity; (*1a*) scanning with a higher resolution in amplitude. The day numbers of the year 1995 are laid off on the abscissa axis; the arrow shows the occurrence time of the Neftegorsk earthquake.

otic systems in the outer and inner shells of the Earth be described by the equations

$$dx/dt = F(x) + K(x, y), \qquad (2)$$

$$dy/dt = G(y) + L(y, x). \qquad (3)$$

The variables x and y are vectors that can have the same or different dimensions, and the functions K and L link the parameters of the systems. We assume that $K \neq 0$ is the coupling coefficient between the atmospheric pressure and strains in the lithosphere, and the feedback coefficient is $L \cong 0$. Then, dynamic changes in the atmosphere will influence phenomena in the lithosphere. It is known that chaotic systems of type (2)–(3) are characterized by synchronization effects, particularly in the region of attractors [Ott, 2002; Pykovsky et al., 2003]. The synchronization of the dynamics of systems can arise and be interrupted; in some time intervals, it can be stable (the Lyapunov exponent is negative) [Gauthier and Bienfang, 1996].

In applications, chaotic systems are often encountered in which the amplitude of vibrations, remaining finite, varies in time irregularly from minimum to maximum, and attractors are represented by cyclic orbits [Rossler, 1976; Sobolev et al., 2005]. Effects of phase synchronization can arise in such chaotic systems [Ott, 2002]. The low frequency variations studied in our paper are apparently of this type. A characteristic curve
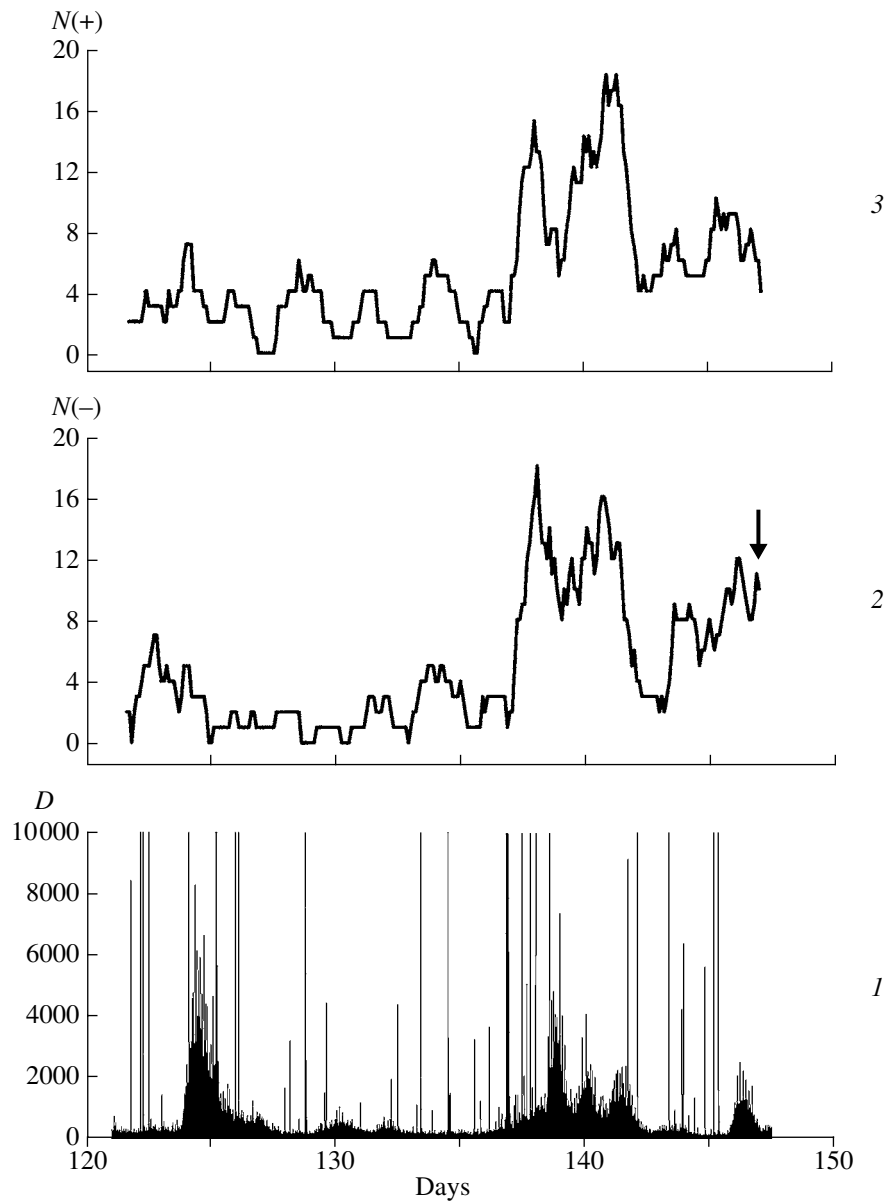
Fig. 10. Comparison of the microseismic level in the range of periods of the order of seconds (*1*) with the daily number of pulses of negative (*2*) and positive (*3*) polarity. The day numbers of the year 1995 are laid off on the abscissa axis; the arrow shows the occurrence time of the Neftegorsk earthquake.

of amplitude variation with time is presented in the upper part of Fig. 11 (see also the plots in Figs. 5 and 8).

Such a system subjected to the effect of periodic vibrations is described by the equation

$$dx/dt = F(x) + KP(\omega t). \qquad (4)$$

Continuing the analogy with systems (2) and (3), we assume that vibrations in the lithosphere are considered and the coefficient K quantifies the extent to which periodic disturbances of the atmospheric pressure influence them. The synchronization interval in the frequency band ω (Fig. 11) is characterized by the following important properties [Ott, 2002]: it is unrecognizable at values of the coupling coefficient K smaller than a certain threshold K_0 and widens with increasing K. We may assume that, with approaching macroinstability (an earthquake), the sensitivity of the metastable region of the lithosphere (the K value) to the atmospheric pressure increases. Under such conditions, it is possible to reveal (within a certain range of periods) sequences of the variations that are the subject of our study.

We considered that they can, in principle, arise due to the interaction of lithospheric and atmospheric processes. External factors might include gravitational, electromagnetic, and other effects. We should also note the effects of phase synchronization of high frequency
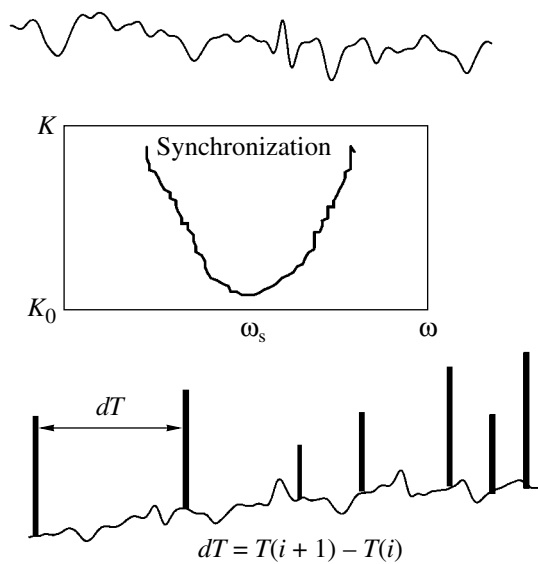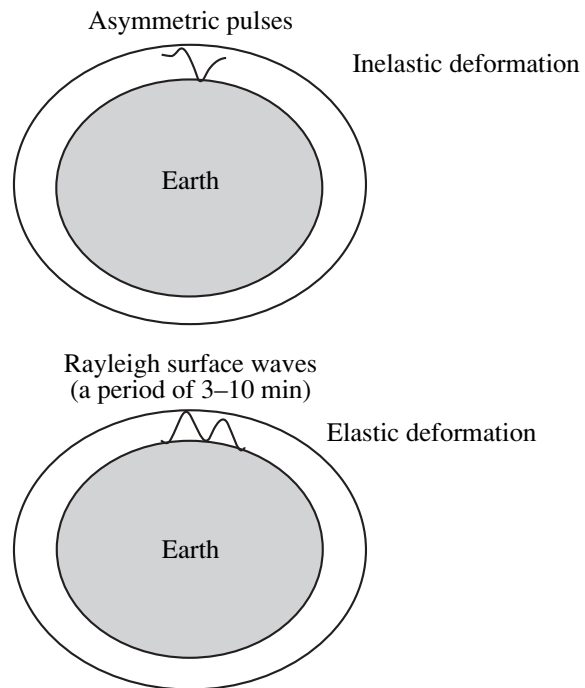
Fig. 11. Diagram illustrating the occurrence of the synchronization effects and pulses in a dynamic system containing chaotic and quasi-periodic components. The upper and lower curves are examples of temporal variations in the vibration amplitude (see explanations in the text).

Fig. 12. Diagram illustrating the occurrence of asymmetric pulses in the lithosphere due to inelastic deformation in the earthquake nucleation region (see explanations in the text).

seismic noises and tides [Saltykov et al., 1997]. It is also possible that the excitation mechanism of the vibrations in question is of the purely lithospheric origin. The occurrence of rhythms is a phenomenon fairly typical of the evolution of nonequilibrium systems [Nikolis and Prigogine, 1977]. An prime example is the "chemical clock" of the type of the Belousov–Zhabotinskii reaction. It is important that the rhythmic variations can have a pulse shape in this case. Note that the variations presented in Figs. 5 and 8 have the velocity dimension (nm/s). In the case of a unipolar pulse, they are evidence for the seismometer response to a ground displacement step several minutes long. The analogy with creep motions along a fault readily suggests itself.

Here, we should emphasize a property of pulsed variations that was mentioned above only casually. In both cases of the Kronotskii and Neftegorsk earthquakes, the records of the Pet and Yss stations, which are the nearest to the earthquake source, were compared with Mag, Yak, Aru, and Obn records obtained at the same time. The epicentral distances of the Pet, Mag, Yss, Yak, Aru, and Obn stations from the Kronotskii earthquake were, respectively, 350, 900, 1670, 2050, 5900, and 6800 km. In the case of the Neftegorsk earthquake, the epicentral distances were (in km) 710 (Yss), 870 (Mag), 1040 (Pet), 1280 (Yak), 5130 (Aru), and 6250 (Obn).

If the vibrations in question with a period of $T = 10$ min were elastic waves, the wavelength under the upper lithosphere–crust conditions would range from 2000 to 4000 km for surface (transverse) and longitudinal waves, respectively. Then, the two to three stations

nearest to the epicenter would be located within a wavelength interval (the near-field zone) and one could expect that the same pulse would be recorded at these stations with a shift of a few minutes. However, the same pulses at adjacent stations could not be clearly identified. A coincidence was observed only for the strongest pulses, as was described in [Sobolev et al., 2005]. Therefore, at the present stage of research, we suggest that the physical origin of the pulses is related to inelastic (pseudoplastic) movements in the sources of forthcoming earthquakes or in the near fault zones. For the Kronotskii earthquake, this can be the subduction zone, and, for the Neftegorsk earthquake, this can be the regional fault extending along Sakhalin Island from the epicenter to the Yss station.

Evolution of the rhythm of pulsed variations. The problem of the origins of the 30–40-min rhythm remains unsolved in terms of both an external influence on a fault zone (synchronization) and an internal mechanism. However, a decrease of the interpulse time (rhythm quickening) was observed. We consider this phenomenon in terms of the dynamics of chaotic systems. A diagram of the occurrence of pulses against the background of oscillations of the type of Eq. (4) is shown in Fig. 11 (the lower plot). Gauthier and Bienfang [1996] showed that, with approaching macroinstability at the transient bubbling stage, synchronization intervals are interrupted by short pulsations of a high

amplitude. The development of macroinstability can increase their recurrence frequency [Ott, 2002]:

$$P(dT) \sim (dT)^{-n}, \qquad (5)$$

where $P(dT)$ is the occurrence probability of interpulse intervals of the length dT and $n > 1$ (i.e., the probability of a short interval is higher). This was demonstrated by studying a relatively simple dynamic system in which a particle in a viscous liquid is subjected to the effects of an electric field and sinusoidal vibration. The situation in the Earth is much more complex, so that this example only indicates that this phenomenon is basically possible.

Asymmetry of pulses. In the sequence of pulses studied in our work, symmetric and asymmetric pulses alternated. By symmetry we mean here approximately equal amplitudes of positive and negative phases of vibration. Figure 3 and curve *2* in Fig. 5 give examples of such pulses. In our case, asymmetric pulses arose more regularly in time and their number increased with approaching the times of the Kronotskii and Neftegorsk earthquakes (Figs. 6, 7, 9, 10). We will consider one of the possible explanations of the asymmetry occurrence. In the laboratory experiments described in [Sobolev and Ponomarev, 1997], samples loaded up to fracture were additionally subjected to sinusoidal stress–strain vibrations. It was established that, with approaching the fracture, receiving ultrasonic sensors recorded a distorted sinusoid in which the amplitude of the extension phase exceeded the amplitude of the compression phase. The effect arose at the inelastic deformation stage, characterized by the deviation of the rheological curve from Hooke's law. The following mechanism provides the most plausible interpretation of the sign of an asymmetric pulse: positive asymmetry (an upward bias) corresponds to compression, while negative asymmetry (a downward bias) corresponds to extension. This is suggested by the direction of the oceanic plate subduction and the position of the seismic stations.

Ekstrom [2001] showed that surface wave trains induced by processes in the atmosphere or by weak earthquakes constantly exist in the lithosphere. Ekstrom considered nearly the same range of periods (200–400 s) as in our study. It is possible to assume (Fig. 12) that vibrations symmetrical under the conditions of an elastic lithosphere (crust) are transformed into asymmetric impulses due to the suppression of one of its phases when the wave crosses a region of inelasticity caused by fracturing or plasticity.

CONCLUSIONS

The analysis of records of broadband seismic stations revealed that, several days before the Kronotskii (the Kamchatka Peninsula) earthquake of $M = 7.7$ and the Neftegorsk (Sakhalin Island) earthquake of $M = 7.0$, pulsed vibrations a few minutes long arose that were separated by time intervals of a few tens of minutes.

The shape asymmetry of pulses characterized by different amplitudes of the phases of positive and negative polarity becomes stronger with approaching the earthquake occurrence time. The recurrence frequency and regularity of asymmetric pulses also increase with approaching earthquake occurrence time.

It is suggested that the origin of this phenomenon is related to the processes of self-organization of the seismic process in a metastable lithosphere and to the synchronization of vibrations in the inner and outer shells of the Earth, whose dynamics includes chaotic and quasi-periodic components.

To elucidate the mechanism responsible for the occurrence of the pulsed vibrations under study, both further experimental observations on a denser network of stations and the development of the theory of nonequilibrium multiphase media are required.

REFERENCES

1. G. Ekstrom, "Time Domain Analysis of Earth's Long-Period Background Seismic Radiation," J. Geophys. Res. **106** (B11), 26 483–26 493 (2001).

2. D. J. Gauthier and J. C. Bienfang, "Intermittent Loss of Synchronization in Coupled Chaotic Oscillators," Phys. Rev. Lett. **77**, 1751–1762 (1996).

3. W. Hardle, *Applied Nonparametric Regression* (Cambridge Univ. Press, Cambridge, 1989; Mir, Moscow, 1993).

4. N. Kobayashi and K. Nishida, "Continuous Excitation of Planetary Free Oscillations by Atmospheric Disturbances," Nature **395**, 357–360 (1998).

5. A. A. Lyubushin, V. F. Pisarenko, V. V. Ruzhich, and V. Yu. Buddo, "Identification of Periodicities in the Seismic Regime," Vulkanol. Seismol., No. 1, 62–76 (1998).

6. S. Mallat, *A Wavelet Tour of Signal Processing* (Academic, San Diego, 1998; Mir, Moscow, 2005) [in Russian].

7. G. Nikolis and I. Prigogine, *Self-Organization in Nonequilibrium Systems* (Wiley, New York, 1977; Mir, Moscow, 1979).

8. E. Ott, *Chaos in Dynamic Systems* (Univ. Press, Cambridge, 2002).

9. A. Pykovsky, et al., *Synchronization. A Universal Concept in Nonlinear Science* (Univ. Press, Cambridge, 2003).

10. O. E. Rossler, "An Equation for Continuous Chaos," Phys. Lett. A **57**, 397–399 (1976).

11. M. A. Sadovsky, *Multidisciplinary Studies of Physics of Earthquakes. An Introduction* (Nauka, Moscow, 1989) [in Russian].

12. V. A. Saltykov, V. I. Sinitsyn, and V. N. Chebrov, "High-Frequency Seismic Noise from Monitoring in Kamchatka," Fiz. Zemli, No. 3, 39–47 (1997) [Izvestiya, Phys. Solid Earth **33**, 205–212 (1997)].

13. G. A. Sobolev, "Microseismic Variations Prior to a Strong Earthquake," Fiz. Zemli, No. 6, 3–13 (2004) [Izvestiya, Phys. Solid Earth **40**, 455–464 (2004)].

14. G. A. Sobolev and A. V. Ponomarev, "Vibrational Effect on the Fracture Process and the Acoustic Regime in a Fault Zone Model," Vulkanol. Seismol., No. 6, 51–57 (1997).

15. G. A. Sobolev, A. A. Lyubushin, and N. A. Zakrzhevskaya, "Synchronization of Microseismic Variations within a Minute Range of Periods," Fiz. Zemli, No. 8, 3–27 (2005) [Izvestiya, Phys. Solid Earth **41**, 599–621 (2005)].

16. T. Tanimoto, J. Um, K. Nishida, and N. Kobayashi, "Earth's Continuous Oscillations Observed on Seismically Quiet Days," Geophys. Res. Lett. **25**, 1553–1556 (1998).

17. V. N. Zharkov and V. P. Trubitsyn, *Physics of Planetary Interiors* (Nauka, Moscow, 1980) [in Russian].